Interaction of the high energy deuterons with the graphite target in the plasma focus devices based on Lee model

M. Akel, S. Alsheikh Salo, Sh. Ismael, S. H. Saw, and S. Lee

Citation: Physics of Plasmas (1994-present) **21**, 072507 (2014); doi: 10.1063/1.4890222
View online: http://dx.doi.org/10.1063/1.4890222
View Table of Contents: http://scitation.aip.org/content/aip/journal/pop/21/7?ver=pdfcov
Published by the AIP Publishing

Interaction of the high energy deuterons with the graphite target in the plasma focus devices based on Lee model

M. Akel,[1,a)] S. Alsheikh Salo,[1] Sh. Ismael,[1] S. H. Saw,[2,3] and S. Lee[2,3,4]
[1]*Department of Physics, Atomic Energy Commission, Damascus, P. O. Box 6091, Syria*
[2]*INTI International University, 71800 Nilai, Malaysia*
[3]*Institute for Plasma Focus Studies, 32 Oakpark Drive, Chadstone VIC 3148, Australia*
[4]*Physics Department, University of Malaya, Kuala Lumpur, Malaysia*

(Received 21 May 2014; accepted 1 July 2014; published online 15 July 2014)

Numerical experiments are systematically carried out using the Lee model code extended to compute the ion beams on various plasma focus devices operated with Deuterium gas. The deuteron beam properties of the plasma focus are studied for low and high energy plasma focus device. The energy spectral distribution for deuteron ions ejected from the pinch plasma is calculated and the ion numbers with energy around 1 MeV is then determined. The deuteron–graphite target interaction is studied for different conditions. The yield of the reaction $^{12}C(d,n)^{13}N$ and the induced radioactivity for one and multi shots plasma focus devices in the graphite solid target is investigated. Our results present the optimized high energy repetitive plasma focus devices as an alternative to accelerators for the production of ^{13}N short lived radioisotopes. However, technical challenges await solutions on two fronts: (a) operation of plasma focus machines at high rep rates for a sufficient period of time (b) design of durable targets that can take the thermal load. © *2014 AIP Publishing LLC*. [http://dx.doi.org/10.1063/1.4890222]

I. INTRODUCTION

Plasma focus device is one of the simplest and low-cost machines in fusion research activities. It has attracted much attention as an intense pulsed source of x-rays, neutrons, high energy fast ion beams, and relativistic electrons.[1–5] Plasma focus devices have been widely used, in the past for manifold applications like x-rays and electron beams lithography,[6] radiography of biological specimens,[7] and as a rich ion source for various material science applications.[8–17] We consider the use of plasma focus devices with sufficient ion energy to produce a number of short lived radioisotopes (SLR) such as ^{13}N, ^{17}F, ^{18}F, ^{15}O, and ^{11}C through either external solid (exogenous method)[18–30] or high atomic number gas (endogenous method)[31–42] targets. These short lived radioisotopes are positron emitter used for positron emission tomography (PET) imaging. Positron emission tomography is an imaging technique that shows the distribution of positron-emitting nuclides in a patient's body. More radioactive material accumulates in areas that have higher levels of chemical activity. Although there are many positron-emitting radiopharmaceuticals, the precise type of radioactive material and its delivery method depend on which organ or tissue is being studied by the PET scan.[28,43] The ^{13}N (half-life $t_{1/2} = 9.97$ min and threshold energy of 0.6 MeV) is a positron emitter when annihilated with electron, consequently, gamma quanta with 511 keV is produced with maximum cross-section of 240 mbarns at 2.3 MeV (Ref. 26) with reasonable cross-section of 100 mbarns above 1 MeV. Nitrogen-13 is used to tag ammonia molecules for PET myocardial perfusion imaging. Usually the practical amount of activities for PET procedure is of the order of 0.368–0.736 GBq. But generally the practical amount of produced radioisotope is usually 4 GBq because of the required time for labeling and purifications in hot cells. In most current facilities, the target is bombarded by protons from a cyclotron.[44,45] Production of short lived radioisotopes has also been demonstrated using femto-second lasers, but such systems are still very expensive. It is desirable to investigate other methods for generating high-energy particles to induce nuclear reactions producing PET radioisotopes such as plasma focus device.[36] With improved plasma focus technology, the cost of production of short live radioisotopes used in medical diagnostics could be lower. Competitive advantages, compared to current systems using cyclotrons, include no neutron radiation, no radio-material waste along the reprocessing line, and possible lower maintenance costs. The $^{12}C(d,n)^{13}N$ reaction is attractive because of its low threshold energy, relatively high cross section, and availability of carbon solid targets, such as graphite and soot. The highest activity of ^{13}N produced in carbon target was reported by Gullickson and Sahlin[19] using 76 kJ discharge energy. They reported production of 160 kBq ^{13}N in one shot. Roshan *et al.*[23] reported production of 40 kBq ^{13}N in a series of 30 shots with 1 Hz repetition rate in a much lower energy device NX2 (1.7 kJ). They expect to produce up to10 MBq with 16 Hz repetition rate in 10 min working time in the future. It is expected to produce much more radioactivity of ^{13}N by higher energy plasma focus devices working at higher discharge repetition rates, up to 16 Hz for which the NX2 was designed to operate at. A proportionality law relating the radioisotope yield to the discharge energy and shot repetition frequency will characterize the appropriate plasma focus for use in this special application. Such a scaling law is not still at hand due to the scarcity of published experimental data. New experimental data from various plasma focus devices can produce interesting results to allow the extension of scaling law for radioisotopes.

[a)]E-mail: pscientific2@aec.org.sy

Moreover, the effects of operational parameters as well as design parameters of a plasma focus device on radioisotope production require much more experimental data to be fully understood. Furthermore, the formed pinch plasma focus parameters and the properties of emitted ion (deuteron) beam (fluence, current densities, energy, ion numbers, etc.) play a key role to produce the SLR. Therefore, the Lee model has been modified based on the virtual plasma diode mechanism proposed by Gribkov *et al.* for studying of the properties of ion beams emitted from plasma focus.[46–50]

In this work, the deuterons beam properties are estimated using modified Lee model code on different plasma focus devices operated with deuterium gas. The energy spectral distribution for deuteron ions is also estimated. The reaction yield of $^{12}C(d,n)^{13}N$ and the radioactivity induced in the graphite target are determined for each studied plasma focus device operated with single and hypothetical repetitive modes.

II. PROCEDURES USED IN THE NUMERICAL EXPERIMENTS

All numerical experiments in this work have been carried out using the following procedures:

1. The Lee model code[48–52] RADPFV5.15FIB has been used to calculate the plasma focus parameters (peak and pinch currents, pinch dimensions and duration, etc.) and the properties of deuteron beam (fluence, flux, current densities and ion numbers, etc.) emitted from various plasma focus devices operated with Deuterium gas.
2. Then, based on the obtained Lee model results, the energy spectral distribution for deuteron ions is calculated for the energy range of 0.01–3 MeV, using the following equation:[18,25,28,53]

$$f(E) = N_i\left[\frac{1-m}{E_{max}^{1-m} - E_{min}^{1-m}}\right].E^{-m} \quad (\text{where } m = 2,\ 3). \qquad (1)$$

3. The ion numbers with energy around 1 MeV is then determined from the energy spectral distribution for deuteron ions and taken into account the radioactivity calculations.
4. For the reaction yield calculations of $^{12}C(d,n)^{13}N$, the ion emission half solid angle of plasma focus $[\Omega_1 = 2\pi(1-\cos\theta_1)\,(sr)]$ and the half solid angle of the target $[\Omega_2 = \pi(\theta_2)^2 = \pi(r/R)^2\,(sr)]$ are determined $(\Omega_2 \le \Omega_1)$, where (r—radius of the target, and R—distance between the target and the tip of the anode). We show that the angular distribution of the deuterons is found to be close to an exponential distribution (i.e., $N_i(\theta_1) \sim \exp(-0.076\theta_1)$.[19,28] Measurements in some other laboratories have also shown that the angular distribution of deuteron intensity is strongly forward peaked with anisotropy exceeding 10^2 (the ratio of deuteron yield in axial and radial directions).[28]
5. Experimental cross-section ($\sigma(E)$) of the reaction $^{12}C(d,n)^{13}N$ is taken from EXFOR database[54] for energy range of 0.6–3.0 MeV, then fitted with the 6-polynomial function as shown in the Figure 1.

After that it is inserted into the following reaction yield equation:

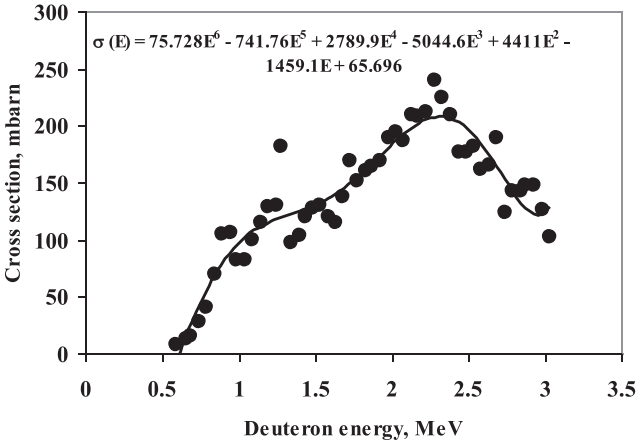

FIG. 1. Cross sections for $^{12}C(d,n)^{13}N$ reaction, taken from the EXFOR database and the fitted curve.

$$\langle y\rangle = \frac{\Omega_2}{\Omega_1}.\left[\frac{1-m}{E_{max}^{1-m} - E_{min}^{1-m}}\right].\int_{E_{min}}^{E_{max}} n.\frac{E^{-m}.\sigma(E)}{\frac{dE}{dx}}.dE, \qquad (2)$$

where n is the graphite target density $(n = 1.129 \times 10^{29}\,m^{-3})$, (dE/dx) is the stopping power of the graphite target and is found to be dE/dx (MeV/m) $= 51232\,E^{-0.71}$ (see Fig. 2) using SRIM code.[55] The integral $\int_{E_{min}}^{E_{max}} n \cdot \sigma(E) \cdot \left(\frac{dE}{dx}\right)^{-1}.dE$ is the probability of the reaction for one deuteron passing a thick target, also named as thick target yield[23,28] (see Fig. 3). In our calculations, the energy loss for energetic ions (required for isotope production) due to interactions with the background gas (deuterium) is too low to be considered and is neglected (For example, the energy loss of a 1 MeV deuteron passing through 30 cm of deuterium gas with 5 Torr pressure is about 20 keV and it is even less for higher energy deuterons).

6. The radioactivity (in Bq) for one shot of plasma focus device induced in the graphite solid target is then written as:[18,25,28]

$$A = N_i\langle y\rangle.\frac{Ln2}{T_{1/2}}. \qquad (3)$$

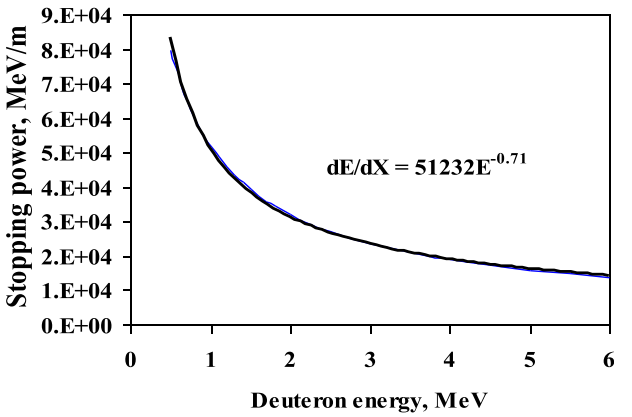

FIG. 2. The stopping power of deuterons in the graphite target and the fitted curve.

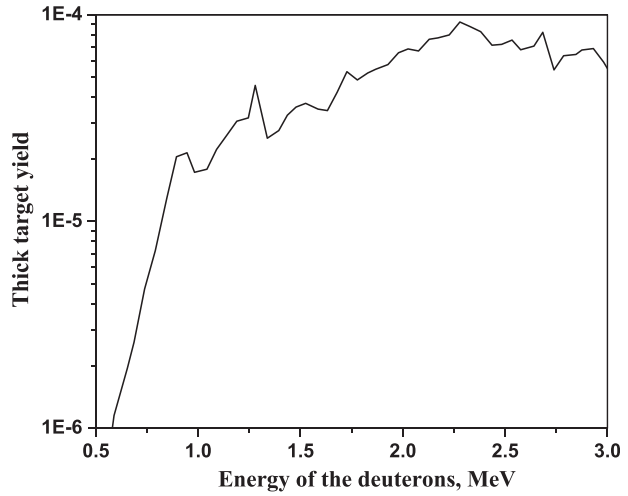

FIG. 3. Thick target yield for the reaction $^{12}C(d,n)^{13}N$ as a function of the deuteron energy.

The $T_{1/2} \sim 10\,\text{min} = 600\,\text{s}$ is the half-life time of radionuclide ^{13}N.

7. Finally, the total radioactivity for repetitive operation mode can be determined by using the following formula:

$$A_\nu = N_i.\langle y\rangle.\nu.\left(1 - e^{-\frac{Ln2}{T_{1/2}}.t}\right), \quad (4)$$

where t is the operation time of plasma focus device, and ν is the frequency of shots.

III. RESULTS AND DISCUSSION

Following the above mentioned procedures, series of numerical experiments were investigated systematically to characterize various plasma focus devices operated with deuterium and to estimate the radioactivity for one shot and multi shots of plasma focus induced in the graphite target under different conditions. First, the plasma focus parameters (peak and pinch currents, pinch dimensions and duration, etc.) and the properties of deuteron beam (fluence, flux, mean ion energy and ion numbers, etc.) emitted from the plasma focus operated with deuterium have been found for selected low and high energy plasma focus devices (see Tables I and II) using modified Lee model[48–52] at the exit of the formed pinch. Generally, at a distance from the pinch to the graphite target, the propagating ion beam will be attenuated by interaction with the medium traversed and also by beam and stream divergence. The deuteron energy spectrum of plasma focus has a wide energy range of 0.01–3 MeV, but only deuterons with energies around 1 MeV can efficiently participate in the reaction $^{12}C(d,n)^{13}N$, so the energetic deuterons numbers were deduced from the ion time-averaged energy spectral distribution (we used Eq. (1) with $m = 3$) of deuterons ejected out of the pinch plasma, taking into account the radioactivity calculations. For studying the plasma focus deuterons-graphite target interactions, we start our numerical experiments with the following assumptions: The deuterons emission half angle of plasma focus $= \theta_1 = 25\,\text{deg} = 0.436\,\text{rad.}$, radius of the graphite target ($r = 2\,\text{cm}$), distance between the graphite target and the tip of the anode ($R = 30\,\text{cm}$), this gives the half angle of the graphite target $= \theta_2 = r/R = 0.067\,\text{rad.} = 3.84\,\text{deg}$. In all our calculations, the half solid angle of the target (Ω_2) is kept smaller than the half solid angle of deuteron emitted from plasma focus (Ω_1) and the angular distribution of the deuteron density was determined and considered to be so small for $\theta_2 = 3.84\,\text{deg}$; therefore at a small emission angles, the deuterons angular distribution was not taken into account. And the energy loss for energetic deuterons (required for isotope production) is also neglected due to its small value. Based on these above mentioned conditions and Lee model results, for

TABLE I. A range of low storage energy plasma focus: deuteron beam characteristics and radioactivity of the reaction $^{12}C(d,n)^{13}N$. The deuterons emission half angle of plasma focus $= \theta_1 = 25\,\text{deg}$, radius of the graphite target ($r = 2\,\text{cm}$), distance from graphite target to tip of anode ($R = 30\,\text{cm}$). The energy of the bank E_0, static inductance L_0, charging voltage V_0, peak current I_{peak}, pinch current I_{pinch}, pinch length z_p, pinch radius r_p, and pinch duration τ are also listed. (Assume spectral distribution index $m = 3$).

Device	PF 400 J (Ref. 48)	ICTP (Ref. 56)	PF 2.2 kJ (Ref. 57)	PF 2.7 kJ (Ref. 29)	NX2 (Ref. 48)	INTI (Ref. 48)	PF II (Ref. 58)
E_0 (kJ)	0.37	2.16	2.22	2.7	2.7	3.4	4.7
L_0 (nH)	40	102	330	70	20	110	45
V_0 (kV)	28	12	25	14	14	15	30
I_{peak} (kA)	129	140	90	185	365	180	361
I_{pinch} (kA)	84	110	61	100	213	122	211
z_p (cm)	0.8	1.4	1.53	1.7	2.8	1.4	2.6
r_p (cm)	0.09	0.14	0.15	0.16	0.31	0.13	0.27
τ (ns)	5.1	10	21.6	15	26	7.6	12.6
Ion fluence ($\times 10^{20}\,m^{-2}$)	2.6	2.8	2.6	2.5	3.2	5.7	1.5
Ion flux ($\times 10^{27}\,m^{-2}\,s^{-1}$)	50.4	28.8	11.9	17.1	12.3	15.6	11.9
Ion number ($\times 10^{14}$)	5.9	15.4	17.63	21.4	95.3	19	34.6
Ion number ($\times 10^{12}$) with energy around 1 MeV	0.11	0.32	0.36	0.43	2	0.4	0.7
Radioactivity for one shot (kBq)	0.06	0.16	0.18	0.22	1.03	0.21	0.36
Total radioactivity with 1 Hz for 600 s (MBq)	0.03	0.07	0.08	0.1	0.443	0.091	0.16
Total radioactivity with 10 Hz for 600 s (MBq)	0.25	0.7	0.8	1	4.5	0.9	1.6
Total radioactivity with 16 Hz for 600 s (MBq)	0.4	1.2	1.3	1.6	7.3	1.5	2.5

TABLE II. A range of high storage energy plasma focus: deuteron beam characteristics and radioactivity of the reaction $^{12}C(d,n)^{13}N$. The deuterons emission half angle of plasma focus $= \theta_1 = 25$ deg, radius of the graphite target (r = 2 cm), distance from graphite target to tip of anode (R = 30 cm). (Assume spectral distribution index m = 3).

Device	PF 10 kJ (Ref. 26)	NX3 (Ref. 48)	DPF78 (Ref. 48)	PF 115 kJ (Ref. 36)	Texas (Ref. 48)	Poseidon (Ref. 48)	PF1000 (Ref. 48)
E_0 (kJ)	10.6	20	31	115.2	126	281	486
L_0 (nH)	120	47	55	120	40	18	33
V_0 (kV)	15	20	60	40	60	60	27
I_{peak} (kA)	319	614	961	970	1509	3205	1846
I_{pinch} (kA)	211	381	444	620	742	1000	862
z_p (cm)	2.92	4.7	5.5	10.4	7.7	11	18.8
r_p (cm)	0.28	0.47	0.62	0.94	0.84	1.22	2.23
τ (ns)	25	38	41	98	77.5	83	255
Ion fluence ($\times 10^{20}$ m^{-2})	4.1	4.9	3.2	6.4	7.8	7	3.9
Ion flux ($\times 10^{27}$ m^{-2} s^{-1})	17	13	7.8	6.7	10	8.4	1.5
Ion number ($\times 10^{14}$)	104	325	390	1771	1700	3300	6100
Ion number ($\times 10^{14}$) with energy around 1 MeV	0.022	0.068	0.083	0.36	0.34	0.7	1.2
Radioactivity for one shot (kBq)	1.2	4	4.5	19	17.7	36	62
Total radioactivity with 1 Hz for 600 s (MBq)	0.5	1.6	1.9	8.1	8	16	27
Total radioactivity with 10 Hz for 600 s (MBq)	5	16	19	81	80	160	270
Total radioactivity with 16 Hz for 600 s (MBq)	8	25	30.1	131	125	250	433

the first time, we proceed our numerical experiments to estimate the yield of the $^{12}C(d,n)^{13}N$ reaction (Eq. (2)), then to find the radioactivity (Eq. (3)) for one shot of plasma focus device induced in the graphite solid target as well as to determine the total radioactivity for plasma focus operated with repetitive mode (Eq. (4)). The obtained results for various plasma focus devices with one and multi-shots are shown in Tables I and II.

It can be noticed that the deuterons numbers generally increase with higher plasma focus energy, and the induced radioactivity in the graphite target has the same trend versus the stored energy of the plasma focus device. The radioactivity from one shot plasma focus ranges from 0.06 kBq (for PF of 0.4 kJ) to 62 kBq (for PF of 500 kJ). Moreover, fixing all previous conditions and taking into account the formed pinch geometry for each device (i.e., distance from the top of the pinch to the graphite target), the radioactivity from one shot plasma focus could be enhanced. As an example for NX2 device, the radioactivity for one shot is 1.03 kBq at target distance 30 cm from the anode, and becomes 1.3 kBq at distance (30—length of the pinch = 30–2.8 = 27.2 cm), i.e., it increases 1.25 times. While for PF1000 device (length of the pinch is 18.8 cm), the radioactivity from one shot increases from 62 kBq to 442 kBq (improvement of 7.2 times). So, we think that the length of the pinch (i.e., start point of the deuteron beam) should be taken into account, especially for good performance and high energy plasma focus devices. Next, numerical experiments to study of the effect of the solid angle graphite target on the induced radioactivity have been investigated. The obtained results for low energy plasma focus at r—radius of the target = 4 cm, and R—distance between the target and the tip of the anode = 10 cm, show that the induced radioactivity for one shot in the graphite target increases by 36 times. While for high energy plasma focus at r = 4 cm and R = 20 cm, the induced radioactivity for one shot increases by 9 times. This means that the correct selection for the solid angle of the graphite target could improve the induced radioactivity. Moreover, there is still scope for optimization of plasma focus parameters (such as anode geometry, inductance, charging voltage, gas pressure, energetic deuteron number, etc.), along with higher repetition rate operation, which could significantly increase the obtained activation. Of course, the parameter space is large and difficult to explore in a systematic way. Higher repetition rate operation is the most straightforward way of increasing the isotope yield. The NX2 device, which is one of the more typical and good performance plasma focus devices, was designed to operate with repetitive mode at 16 Hz for periods of 600 s with a cooled anode.[59] So, we continue our numerical experiments on selected plasma focus devices with various repetition modes (1, 10, 16, 100, 1000 Hz) to find the induced radioactivity versus shots frequency. For example, the obtained results show that the induced radioactivity from NX2 (2.7 kJ) device increases from 1.03 kBq (for one shot) to 7.3 MBq and 450 MBq for 16 Hz and 1 kHz, respectively, for 600 s operation period, while for NX3 (20 kJ) device increases from 4 kBq (for one shot) to 25 MBq and 1600 MBq for 16 Hz and 1 kHz, respectively, and from PF1000 (486 kJ) device increases from 62 kBq (for one shot) to 433 MBq and 27000 MBq for 16 Hz and 1 kHz, respectively, for 600 s operation period. Our results with repetitive rate plasma focus indicate that high frequency high energy plasma focus devices are required for generation of the practical amount of Nitrogen-13 used to tag ammonia molecules for PET myocardial perfusion imaging. It is noted that in the present state of the art and technology, 100 shots/s plasma focus has yet to be achieved even for a 1 kJ focus, as can be surmised from the recent review paper by Krishnan.[60]

The numerical experiments are repeated with the ion time-average energy spectral distribution (Eq. (1) with m = 2) of deuterons ejected out of the pinch plasma. The

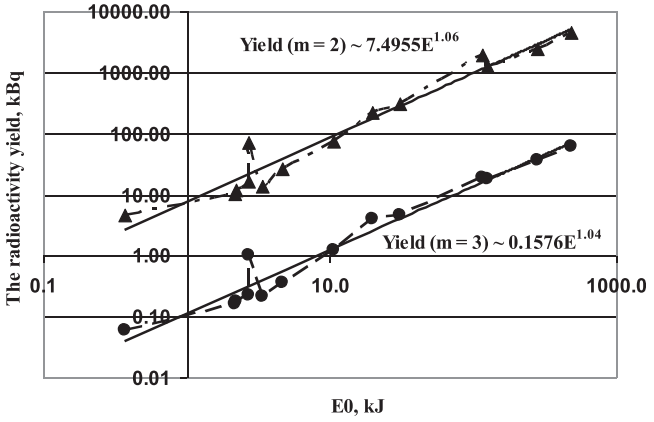

FIG. 4. The scaling law for the ^{13}N yield versus the stored energy of the studied plasma focus devices for one shot with spectral distribution index m = 2 and 3.

results show that the induced radioactivity increases dramatically with smaller values of m. Finally, we would like to emphasize that recently, there are scant experimental data on which to base the scaling law for the ^{13}N isotope yield versus bank energy of the plasma focus devices. Therefore, based on our numerical experiments, we present the scaling law for the ^{13}N yield versus the stored energy of the studied plasma focus devices for one shot (see Fig. 4), where the jumps on the yield curves are for the high-performance low-inductance NX2 (2.7 kJ) device and the jumps on the higher energy devices are for the higher voltage high-performance devices.

The results we obtained for Tables I and II assume a spectral distribution index m = 3. We chose m = 3 because that value of m gives us an agreement between our NX2 computed yield and the experimental results obtained by Roshan *et al.*[23] On the other hand, if the spectral distribution were such as to be better represented by m = 2, the radioactivity yields would improve by a factor of about 100 (see Fig. 4). We note that the results of Gullickson and Sahlin[19] (production of 160 kBq ^{13}N in one shot at 76 kJ plasma focus stored energy) would indicate that m is closer to the value of 2 than 3. That would improve considerably the potential of this technology suggesting that the NX3 (at 20 kJ) could reach 2.5 GBq at 25 Hz sustained over a period of 600 s; although this would still be beyond the reach of present-day plasma focus devices.

As mentioned earlier placing the target closer could significantly improve the yield. We need to note however that the target could be placed no nearer than 5 times the radius of the anode from consideration of the proper formation of the pinch as well as the limit on heat load that the target is able to take. With increased repetitive rates, the heat load effect would be correspondingly more severe. New target designs are needed to handle these large heat loads. Our calculations in this paper provide useful guidelines for development of targets from the viewpoint of heat dissipation requirements. If such designs become available, our calculations indicate the plasma focus could be useful for irradiation of carbon for SLR production. The use of curved targets to take advantage of upward, side-on and backward high energy deuterons[61] could also be considered to improve the yield. A further improvement in this respect could possibly be to use high voltage plasma focus (100 kV or higher), which could produce a higher ratio of high energy ions.

Furthermore, the numbers produced by these calculations could also be useful for the use of plasma focus machines in other applications such as fast ion beam diagnostics and radiation material science.

IV. CONCLUSION

The modified Lee model code has been used to study the deuteron beams on various low and high plasma focus devices operated with deuterium gas. The energy spectral distribution for deuteron ions ejected from the pinch plasma is calculated with m = 2, 3. The deuteron–graphite target interaction has been studied taking into account the length of the pinch and for different solid angle of the target conditions. The yield of the reaction ^{12}C(d,n)^{13}N and the induced radioactivity in the graphite solid target for one and multi shots plasma focus devices have been investigated. The scaling law for the ^{13}N yield versus the stored energy of the studied plasma focus devices for one shot is found. The numerical experiments show that optimized plasma focus devices with sufficient high energy operating with repetition mode for a certain period could be a potential source of producing clinically useful quantities of ^{13}N and other short-lived isotopes. Using an example of a 20 kJ plasma focus, our results indicate that at least 25 Hz rep rate sustained over a 600 s run needs to be achieved. Such a level of power of plasma focus operation has yet to be demonstrated. This conclusion is consistent with the recent discussions of Roshan *et al.*[62] Moreover, other technical difficulties include on-target heat loads, which require new target designs as yet unavailable. However, independently of the application of our work to the consideration of SLR production, the numbers produced by these calculations could act as guidelines to the use of plasma focus machines in other applications such as fast ion beam diagnostics and radiation material science.

ACKNOWLEDGMENTS

The authors thank the Reviewer of this paper for valuable suggestions to balance the presentation of the key points of the paper. We would like to thank Director General of AECS for encouragement and permanent support. M. Akel would also like to thank Dr. Muthanna Ahmad for the valuable discussion related to SRIM code. S. Lee acknowledges UM.S/625/3/HIR/43 and UMRG102/10AFR.

[1]Y. Kato, I. Ochiai, Y. Watanabe, and S. Murayama, J. Vac. Sci. Technol. B **6**, 195 (1988).
[2]R. Lebert, W. Keff, and D. Rothweiler, J. X-ray Sci. Technol. **6**, 107 (1996).
[3]H. Asai and I. Ueno, Fusion Eng. Des. **7**, 335 (1989).
[4]W. L. Harries, J. H. Lee, and D. R. Mcfarland, Plasma Phys. **20**, 95 (1978).
[5]J. R. Smith, C. M. Luo, M. J. Rhee, and R. F. Schneider, Phys. Fluids **28**, 2305 (1985).
[6]P. Lee, X. Feng, G. Zhang, M. Liu, and S. Lee, Plasma Sources Sci. Technol. **6**, 343 (1997).

[7]M. F. Castillo, M. M. Milanese, R. L. Moroso, J. O. Pouzo, and M. A. Santiago, IEEE Trans. Plasma Sci. **29**, 921 (2001).
[8]M. Sadiq, S. Ahmad, M. Shafiq, and M. Zakaullah, Nucl. Instrum. Methods Phys. Res. B **252**, 219 (2006).
[9]R. S. Rawat, W. M. Chew, P. Lee, T. White, and S. Lee, Surf. Coat. Technol. **173**, 276 (2003).
[10]M. Hassan, R. Ahmad, A. Qayyum, G. Murtaza, A. Waheed, and M. Zakaullah, Vacuum **81**, 291 (2006).
[11]M. Hassan, A. Qayyum, R. Ahmad, G. Murtaza, and M. Zakaullah, J. Phys. D: Appl. Phys. **40**, 769 (2007).
[12]S. R. Mohanty, N. K. Neog, H. Bhuyan, R. K. Rout, R. S. Rawat, and P. Lee, Jpn. J. Appl. Phys., Part 2 **46**, 3039 (2007).
[13]B. B. Nayak, B. S. Acharya, S. R. Mohanty, T. K. Borthakur, and H. Bhuyan, Surf. Coat. Technol. **145**, 8 (2001).
[14]J. Feugeas, G. Grigioni, G. Sanches, and A. R. DaCosta, Surf. Eng. **14**, 62 (1998).
[15]J. Piekoszewski, B. Sartowska, L. Waliś, Z. Werner, M. Kopcewicz, F. Prokert, J. Stanisławski, J. Kalinowska, and W. Szymczyk, Nukleonika **49**(2), 57–60 (2004).
[16]M. J. Marques, J. Pina, A. M. Dias, J. L. Lebrun, and J. Feugeas, Surf. Coat. Technol. **195**, 8 (2005).
[17]H. Kelly, A. Lepone, A. Márquez, D. Lamas, and C. Oviedo, Plasma Sources Sci. Technol. **5**, 704 (1996).
[18]B. Bienkowska, S. Jednorog, I. M. Ivanova-Stanik, M. Scholz, and A. Szydowski, Acta Phys. Slovaca **54**(4), 401–407 (2004).
[19]R. L. Gullickson and H. L. Sahlin, J. Appl. Phys. **49**(3), 1099–1105 (1978).
[20]Y. Yamada, Y. Kitagawa, and M. Yokoyama, J. Appl. Phys. **58**(1), 188–192 (1985).
[21]V. Nardi, L. Bilbao, J. S. Brzosko, C. Powell, D. Zeng, A. Bortolotti, F. Mezzetti, and B. V. Robouch, IEEE Trans. Plasma Sci. **16**(3), 374–378 (1988).
[22]M. V. Roshan, R. S. Rawat, A. Talebitaher, R. Verma, P. Lee, and S. V. Springham, Phys. Lett. A **373**(41), 3771–3774 (2009).
[23]M. V. Roshan, S. V. Springham, R. S. Rawat, and P. Lee, IEEE Trans. Plasma Sci. **38**(12), 3393–3397 (2010).
[24]M. V. Roshan, R. S. Rawat, A. Talebitaher, R. Verma, P. Lee, S. V. Springham *et al.*, J. Plasma Fusion Res. SERIES **8**, 1273–1276 (2009).
[25]S. M. Sadat kiai, M. Elahi, S. Adlparvar, E. Shahhoseini, S. Sheibani, H. Ranjberakivaj, S. Alhooie, A. Safarien, S. Farhangi, N. Aghaei, S. Amini *et al.*, J. Fusion Energy **29**, 421–426 (2010).
[26]S. M. Sadat kiai, S. Adlparvar, S. Sheibani, M. Elahi, A. Safarien, S. Farhangi, A. A. Dabirzadeh, M. M. Khalaj, Y. Vosoughi, A. Moslehi, S. Shafiei *et al.*, J. Fusion Energy **30**(2), 111–115 (2011).
[27]M. Scholz, B. Bienkowska, and V. A. Gribkov, Czechoslovak J. Phys. **52**, D85–D92 (2002).
[28]B. Shirani and F. Abbasi, J. Fusion Energy **32**(2), 235–241 (2013).
[29]B. Shirani, F. Abbasi, and M. Nikbakht, Appl. Radiat. Isotopes **74**, 86–90 (2013).
[30]V. A. Gribkov, A. V. Dubrovsky, M. Scholz, S. Jednorog, L. Karpiński, K. Tomaszewski, M. Paduch, R. Miklaszewski, V. N. Pimenov, L. I. Ivanov, E. V. Dyomina, S. A. Maslyaev, and M. A. Orlova, Nukleonika **51**(1), 55–62 (2006).
[31]E. Angeli, A. Tartari, M. Frignani, V. Molinari, D. Mostacci, F. Rocchi, and M. Sumini, Nucl. Technol. Radiat. Prot. **20**(1), 33–37 (2005).
[32]E. Angeli, A. Tartari, M. Frignani, D. Mostacci, F. Rocchi, and M. Sumini, Appl. Radiat. Isotopes **63**, 545–551 (2005).
[33]J. S. Brzosko and V. Nardi, Phys. Lett. A **155**(2–3), 162–168 (1991).
[34]J. S. Brzosko, V. Nardi, J. R. Brzosko, and D. Goldstein, Phys. Lett. A **192**, 250–257 (1994).
[35]J. S. Brzosko, K. Melzacki, C. Powell, M. Gai, R. H. France, J. E. McDonald, G. D. Alton, F. E. Bertrand, and J. R. Beene, in *16th International Conference on Application of Accelerators in Research and Industry* (2001), pp. 277–280.
[36]S. F. Haghani, A. Sadighzadeh, A. Talaei, A. A. Zaeem, S. M. Sadat Kiai, A. Heydarnia, and V. Damideh, J. Fusion Energy **32**(4), 480–487 (2013).
[37]A. A. Zaeem, S. Mahmood Sadat Kiai, M. Sedaghatizade, S. Adlparvar, and S. Sheibani, J. Fusion Energy **28**, 268–274 (2009).
[38]M. Sumini, D. Mostacci, F. Rocchi, M. Frignani, A. Tartari, E. Angeli, D. Galaverni, U. Coli, B. Ascione, and G. Cucchi, Nucl. Instrum. Methods Phys. Res. A **562**, 1068–1071 (2006).
[39]M. Sumini, D. Mostacci, F. Rocchi, S. Mannucci, A. Tartari, and E. Angeli, *IEEE Nuclear Science Symposium Conference Record, N24-378* (2007), pp. 637–1642.
[40]A. Talaei, S. M. Sadat Kiai, and A. A. Zaeem, Appl. Radiat. Isotopes **68**, 2218–2222 (2010).
[41]V. Razazi and R. M. Gharehbagh, in *Proceedings of the 17th Iranian Conference of Biomedical Engineering (ICBME2010), 3–4 November, Isfahan, Iran, 2010*.
[42]S. M. Sadat Kiai, S. Adlparvar, S. Adlparvar, S. Sheibani, M. Elahi, A. Safarien, S. Farhangi, A. A. Dabirzadeh, M. M. Khalaj, Y. Vosoughi, A. Moslehi, S. Shafiei *et al.*, J. Fusion Energy **30**(6), 459–461 (2011).
[43]S. Castillo, *Medical and Statistical Review of ^{13}N Ammonia Positron Emission Tomography* (1999).
[44]J.-M. Le Goff, in CERN, A very low energy cyclotron for PET isotope production, European Physical Society, Technology and innovation workshop, Erice, 22–24 October, 2012.
[45]P. W. Schmor, "Review of cyclotrons used in the production of radioisotopes for biomedical applications, FRM2CIO01," in *Proceedings of CYCLOTRONS, Lanzhou, China* (2010), pp. 419–424.
[46]V. A. Gribkov, A. Banaszak, B. Bienkowska, A. V. Dubrovsky, I. Ivanova-Stanik, L. Jakubowski, L. Karpinski, R. A. Miklaszewski, M. Paduch, M. J. Sadowski, M. Scholz, A. Szydlowski, and K. Tomaszewski, J. Phys. D: Appl. Phys. **40**, 3592 (2007).
[47]V. N. Pimenov, E. V. Demina, S. A. Maslyaev, L. I. Ivanov, V. A. Gribkov, A. V. Dubrovsky, Ü. Ugaste, T. Laas, M. Scholz, R. Miklaszewski, B. Kolman, and A. Tartari, Nukleonika **53**(3), 111 (2008).
[48]S. Lee and S. H. Saw, Phys. Plasmas **19**, 112703 (2012).
[49]S. Lee and S. H. Saw, Phys. Plasmas **20**, 062702 (2013).
[50]M. Akel, S. Alsheikh Salo, S. H. Saw, and S. Lee, J. Fusion Energy **33**(2), 189–197 (2014).
[51]S. Lee, J. Fusion Energy **33**(4), 319–335 (2014).
[52]S. Lee, Radiative Dense Plasma Focus Computation Package: RADPF. http://www.plasmafocus.net; http://www.intimal.edu.my/school/fas/UFLF/ (archival websites) (2014).
[53]G. Sanchez and J. Feugeas, J. Phys. D: Appl. Phys. **30**, 927–936 (1997).
[54]R. W. Michelmann, https://www-nds.iaea.org/exfor/exfor.htm (2014).
[55]See www.srim.org for the stopping and range of ions in matter.
[56]M. A. I. Elgarhy, "Plasma focus and its applications," M.Sc. Thesis (Cairo, 2010).
[57]S. R. Mohanty, H. Bhuyan, N. K. Neog, R. K. Rout, and E. Hotta, Jpn. J. Appl. Phys., Part 1 **44**(7A), 5199 (2005).
[58]H. Kelly and A. Marquez, Plasma Phys. Controlled Fusion **38**, 1931–1942 (1996).
[59]S. Lee, P. Lee, G. Zhang, X. Feng, V. A. Gribkov, L. Mahe, A. Serban, and T. K. S. Wong, IEEE Trans. Plasma Sci. **26**, 1119 (1998).
[60]M. Krishnan, IEEE Trans. Plasma Sci. **40**(12), 3189–3221 (2012).
[61]M. V. Roshan, P. Lee, S. Lee, A. Talebitaher, R. S. Rawat, and S. V. Springham, Phys. Plasmas **16**, 074506 (2009).
[62]M. V. Roshan, S. Razaghi, F. Asghari, R. S. Rawat, S. V. Springham, P. Lee, S. Lee, and T. L. Tan, Phys. Lett. A **378**(30–31), 2168–2170 (2014).